# *Trypanosoma cruzi*: effect and mode of action of nitroimidazole and nitrofuran derivatives

Juan Diego Maya[a], Soledad Bollo[b], Luis J. Nuñez-Vergara[b], Juan A. Squella[b], Yolanda Repetto[a], Antonio Morello[a], Jacques Périé[c], Gérard Chauvière[c,*]

[a]*Faculty of Medicine, ICBM, Program of Molecular and Clinical Pharmacology, University of Chile, P.O. Box 70086, Santiago 7, Chile*
[b]*Laboratory of Bioelectrochemistry, Faculty of Chemical & Pharmaceutical Sciences, University of Chile, Santiago, Chile*
[c]*Groupe de Chimie Organique Biologique, Université Paul Sabatier, UMR-CNRS 5068, Toulouse, France*

**Abstract**

With the aim of determining the actual target(s) of nitro-group bearing compounds considered as possible leads for the development of drugs against Chagas' disease, we studied in parallel nitrofurans and nitroimidazoles. We investigated nine representative compounds for the following properties: efficacy on different *Trypanosoma cruzi* strains, redox cyclers, inhibition of respiration, production of corresponding nitroso derivatives and intracellular thiol scavengers. Our results indicate that nifurtimox and related compounds act as redox cyclers, whereas the most active in the series, the 5-nitroimidazole megazol essentially acts as thiol scavenger particularly for trypanothione, the cofactor for trypanothione reductase, an essential enzyme in the detoxification process.

*Keywords:* Nitroheterocycles; *Trypanosoma cruzi*; Redox cycling; Intracellular trypanothione scavengers; Respiration inhibitors; Thiols depletion

## 1. Introduction

*Trypanosoma cruzi* is the etiological agent of Chagas' disease, a chronic illness affecting many people in Latin America [1]. Currently, this pathology is treated with nitroheterocyclic agents such as nifurtimox and benznidazole. These two drugs are effective against the circulating form of the parasite (trypomastigotes) during the acute phase of the disease, but not during the chronic stage. Additionally, they produce serious adverse effects including mutagenesis [2,3], if used in long-term therapy. There are also differences in sensitivity between the different strains of the parasite [4]. A characteristic ESR spectrum corresponding to the nitro-anion radical appears when nifurtimox is added to intact *T. cruzi* cells; also, $H_2O_2$ is released to the suspending medium [5–7]. These and other experiments [8,9] suggest that intracellular reduction of nifurtimox followed by redox cycling, yielding $O_2^{\bullet -}$ and $H_2O_2$ is the mode of action of this compound against *T. cruzi*.

A weak signal in the ESR spectrum, corresponding to the nitro-anion radical appears with the addition of benznidazole to NADPH-containing homogenates of *T. cruzi* [7]. Benznidazole does not stimulate $O_2^{\bullet -}$ and $H_2O_2$ generation under the same experimental conditions [10]. Benznidazole inhibits the growth of *T. cruzi* at concentrations that do not stimulate $O_2^{\bullet -}$ and $H_2O_2$ production. This result indicates that the trypanocidal effect of benznidazole does not depend on oxygen radicals as with nifurtimox [10]. Probably reduced metabolites of benznidazole are involved through covalent binding to macromolecules in its trypanocidal and toxic effects [5,11–14].

Megazol [1-methyl-2-(5-amino-1,3,4-thiadiazole)-5-nitroimidazole] is a nitroheterocyclic derivative with antibacterial and antiparasitic activity particularly against trypanosomes [15,16]. The combination of megazol with suramin [17–19] or melarsoprol [20] in the treatment of *T. brucei* infections potentiates its trypanocidal effect. Under experimental conditions, megazol can generate

*E-mail address:* chauvier@cict.fr (G. Chauvière).

*Abbreviations:* DMF, dimethylformamide; DMSO, dimethylsulfoxide; THF, tetrahydrofuran; ITBA, iodide tetrabutylammonium; EDTA, ethylenediamine tetraacetic acid; HEPPS, *N*-(2-hydroxyethyl)-1-piperazine -*N*′-3-propane sulfonic acid; GSH, glutathione; $T(SH)_2$, trypanothione; Ln, natural logarithm; $k_c$, culture growth constant; $E_{pc}$, reduction cathodic peak potential.

oxygen redox cycling [21] at high concentration but protein synthesis inhibition is suggested as its anti-*T. cruzi* mode of action [22]. Because of its efficacy against several strains of *T. cruzi* of diverse sensitivity, it has a potential role in treatment of Chagas' disease. However, megazol has shown mutagenicity [23] at least according to the Ames assay; for this reason, it is necessary to re-evaluate this mutagenicity using more recent assays and to develop nitroimidazoles with similar trypanocidal activity but lower mutagenic profiles. RO150216, other nitroimidazole derivative, has been shown to be effective in inhibiting the culture growth of different strains of the African trypanosome [24], and *in vivo* using various animal models [25].

To get more information on how these different compounds may act and with the aim to define in a second step other possible structures, the present work was undertaken by including in the same study and according to the same protocol several nitroimidazoles and nitrofurans derivatives shown in Fig. 1. These compounds were considered in a parallel study for their action on different strains on *T. cruzi* and their effect on respiration inhibition, redox potential, redox cycling properties and effect as thiol scavengers particularly for trypanothione and glutathione.

## 2. Materials and methods

### 2.1. Chemistry

Nifurtimox (3-methyl-*N*-[(5-nitro-2-furanyl)-methylene]-4-thiomorpholinamine-1,1-dioxide) was provided by Bayer Laboratories, RO150216 (2-(dimethylamino)-4′-[(1-methyl-2-nitroimidazole-5-yl)methoxy]acetanilide) and benznidazole (*N*-benzyl-2-nitroimidazole-1-acetamide) from Hoffman LaRoche; megazol (2-amino-5-(1-methyl-5-nitro-2-imidazolyl)-1,3,4-thiadiazole) and other 5-nitro imidazoles and nitrofurans (Fig. 1) were synthesized from the corresponding 2-cyano-5-nitroheterocycle by condensation, in trifluoroacetic acid, with thiosemicarbazide to generate the thiadiazole ring or with semicarbazide for the oxadiazole ring following a method previously described [26].

Melting points were determined on an electrothermal capillary melting point apparatus and were uncorrected. $^{1}H$ and $^{13}C$ NMR spectra were recorded, respectively on Bruker AC80 (80 MHz) and AC200 (50 MHz). All chemical shifts are reported in ppm relative to TMS as internal standard. Mass spectra were run on a Nermag R1010 spectrometer at P. Sabatier University. All chemicals were purchased from Aldrich or Fluka and were used without extra purification.

DMF and DMSO were dried by stirring over 4 Å molecular sieves. THF was distilled over sodium in the presence of benzophenone ketyl as indicator prior to use. Reactions and column chromatographic separations were followed by thin layer chromatography using silicagel (with 254 nm fluorescent indicator) on aluminum plates.

### 2.2. Megazol: 1-methyl-2-(5-amino-1,3,4-thiadiazole)-5-nitroimidazole

Thiosemicarbazide (2.1 g, 23 mmol) mixed with 1-methyl-2-cyano-5-nitroimidazole (3.28 g, 22 mmol) were

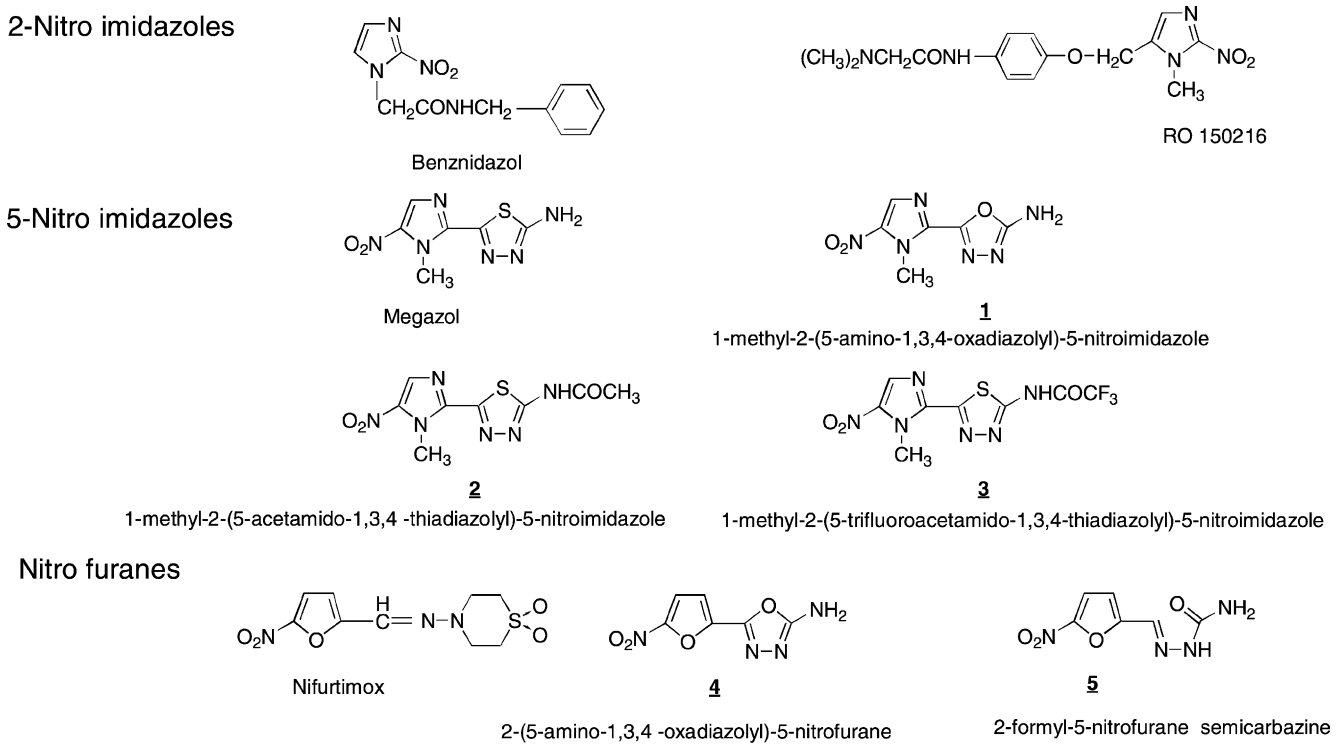


Fig. 1. Chemical structures of the nitroheterocyclic compounds.

heated at 60° in trifluoroacetic acid (10 mL) for 15 hr. The resulting solution was poured into ice water (20 mL) and neutralized with sodium hydrogenocarbonate. The yellow precipitate formed was filtered on a sintered glass filter, washed with water (2 × 5 mL), and dried under vacuum, to give after crystallization in acetone, megazol (2.5 g, 11 mmol, 50% yield); m.p. 270°; $^1$H NMR (DMSO-$d_6$, 80 MHz): 4.32 (s, 3H, $NCH_3$); 7.8 (b, 2H, $NH_2$); 8.2 (s, 1H). $^{13}$C NMR (DMSO-$d_6$, 50 MHz): 35.00 (s, $NCH_3$); 133.1 (C4); 140.1 (C5); 141.4 (C2); 148.2(C2*); 169.9 (C5*). Mass spectrometry: (EI) *m/z* 227 ($M^+ + 1$, 80%). Anal. calc. for $C_6H_6N_6O_2S$: C, 31.53; H, 2.67; N, 37.15. Found: C, 31.64; H, 2.62; N, 36.41.

### 2.3. 1-Methyl-2-(5-amino-1,3,4-oxadiazolyl)-5-nitroimidazole (see Fig. 1, compound **1**)

2-Cyano-1-methyl-5-nitroimidazole (600 mg, 4 mmol) and semicarbazide hydrochloride (500 mg, 4.5 mmol) were mixed in 10 mL of trifluoroacetic acid and refluxed at 70° for 15 hr. The solution was then poured into ice water (10 mL) and carefully neutralized with sodium bicarbonate. The yellow solid formed was filtered and washed with diethyl ether and water. After crystallization in an ethanol/water mixture (2/1 v/v) compound **1** was obtained (420 mg, 50% yield); m.p. 288°, $^1$H NMR (DMSO-$d_6$, 80 MHz): 4.25 (s, $NCH_3$); 7.94 (s, $NH_2$); 8.11 (s, H4); $^{13}$C NMR (DMSO-$d_6$, 50 MHz): 34.53 ($NCH_3$); 130.65 (C4); 140.05 (C5); 141.34 (C2); 157 (C2′); 159.77 (C5′). Anal. calc. for $C_6H_6N_6O_3$: C, 34.29; H, 2.88; N, 39.99. Found: C, 33.79; H, 3.05%.

### 2.4. 1-Methyl-2-(5-acetamido-1,3,5-thiadiazolyl)-5-nitroimidazole (see Fig. 1, compound **2**)

Acetyl chloride (2 mL) was added by syringe through a septum cap on megazol (226 mg, 1 mmol) to 30 mL of anhydrous THF under argon. The mixture was stirred at room temperature for 3 hr. Then the THF was evaporated under vacuum. The residual solid was washed with water, then recrystallized in ethanol/acetone 2/1, to obtain compound **2** (160 mg, 60% yield). $^1$H NMR (DMSO-$d_6$, 80 MHz): 2.24 (s, $COCH_3$); 4.39 (s, $NCH_3$); 8.25 (s, H4); $^{13}$C NMR (DMSO-$d_6$, 50 MHz): 22.33 ($CH_3CO$); 35.23 ($CH_3N$); 133.09 (C4); 140.6 (C2); 141.04 (C5); 153.93 (CONH); 159.74 (C2′); 169.17 (C′).

### 2.5. 1-Methyl-2-(5-trifluoromethylacetamido-1,3,5-thiadiazolyl)-5-nitroimidazole (see Fig. 1, compound **3**)

To megazol (226 mg, 1 mmol) suspended in THF (5 mL) was added trifluoracetic anhydride (2 mL); the suspension dissolved instantly. After 5 min at room temperature, THF and trifluoroacetic anhydride were evaporated under vacuum, and a saturated solution of sodium hydrogenocarbonate was added (3 mL) and then acetone (5 mL). The yellow solid formed was filtered and recrystallized in acetone/water 1/1 (300 mg, 90% yield) $^1$H NMR (DMSO-$d_6$, 80 MHz): 4.54 (s, $NCH_3$); 8.17 (s, H4). $^{13}$C NMR (DMSO-$d_6$, 50 MHz): 35 ($NCH_3$); 117 (q, CF3); 132.9 (C4); 140 (C2); 141 (C2′); 167.7 (CO); 170 (CS). Mass spectrometry: (DCI/$NH_3$) *m/z* 323 ($M^+ + 1$, 60%) 340 ($M^+ + NH_3$, 50%).

### 2.6. 2-(5-Amino-1,3,4-oxadiazolyl)-5-nitrofuran (see Fig. 1, compound **4**)

2-Carbonitrile-5-nitrofuran (700 mg, 5 mmol) and semicarbazide hydrochloride (560 mg, 5 mmol) diluted in trifluoroacetic acid (20 mL) were stirred at 60° for 15 hr; then the cold solution (0°) was carefully neutralized with sodium bicarbonate, and the orange solid obtained was filtered, washed with water and dried under vacuum, to give compound **4** (450 mg, 45% yield); m.p. 240°, $^1$H NMR (DMSO-$d_6$, 80 MHz): 6.33 (s, $NCH_2$); 7.30 (d, H4); 7.80 (d, H3); $^{13}$C NMR (DMSO-$d_6$, 50 MHz): 111.3 (C3); 140 (C2); 114.9 (C4); 133.5 (C2); 150.6 (C5); 150.8 (C′2); 157.0 (C′5). Mass spectrometry: (DCI/$NH_3$) *m/z* 231 ($M^+ + 2NH_3$, 100%).

### 2.7. 2-Formyl-5-nitrofuran-semicarbazine (see Fig. 1, compound **5**)

Semicarbazide hydrochloride (444 mg, 4 mmol) dissolved in DMSO (5 mL) was added to sodium hydride (110 mg, 4 mmol) suspended in DMSO (3 mL). After 5 min, when all hydrogen had evolved, 5-nitrofuran-2-carboxaldehyde (570 mg, 4 mmol) diluted in DMSO (2 mL) was added. After 18 hr at room temperature, the brown solution was poured into water (50 mL). The dark precipitate was filtered, and then purified after dissolving in acetone by flash chromatography ($CH_2Cl_2$/methanol: 90/10) to give compound **5** (400 mg, 55% yield); m.p. 240°, $^1$H NMR (DMSO-$d_6$, 80 MHz): 6.57 (s, NH); 7.22 (d, H4); 7.77 (d, H3); 10.76 (s, CH=N). $^{13}$C NMR (DMSO-$d_6$, 50 MHz): 112.0 (C4); 115.1 (C3); 127.3 (CH=N); 151.1 (C2); 150.0 (C5); 155.8 ($CONH_2$). Mass spectrometry: (DCI/$NH_3$) *m/z* 216 ($M^+ + 18$, 100%).

### 2.8. Assays on cultures

#### 2.8.1. Parasites and culture growth inhibition

A suspension of 3 × $10^6$ *T. cruzi* epimastigotes per mL, from Tulahuén and LQ strains and CL-Brener clone, were cultured at 28° in monophasic Diamond's culture medium supplemented with 4 μM of hemin [27]. Inactivated bovine calf serum at a final concentration of 4% was added. Drugs dissolved in DMSO (final concentration of 1%) were added to the culture media to give 0.5–100 mM final concentrations. Parasite growth was followed by nephelometry for 7–10 days [28,29]. Nephelometry readings were directly proportional to the concentration of parasites. No toxic effect of DMSO alone was observed.

The growth culture constant ($k_c$) for each drug concentration employed was calculated using an exponential epimastigote growth curve (regression coefficient $> 0.97$, $P < 0.05$). The slope resulting from plotting the natural logarithm (Ln) of the nephelometry reading vs. time, in hours, corresponds to the $k_c$ ($hr^{-1}$). The $IC_{k_c50}$ is defined as the drug concentration needed to diminish the $k_c$ in 50%; it is calculated by lineal regression analysis from the $k_c$ values and the concentrations used; $80 \times 10^6$ parasite cells correspond to 1 mg protein or 12 mg of fresh weight.

*2.8.2. Oxygen uptake*

Tulahuén strain *T. cruzi* epimastigotes were harvested by 500 *g* centrifugation, followed by washing and re-suspension in 0.05 M sodium phosphate buffer, pH 7.4, containing 0.107 M sodium chloride. Respiration measurements were carried out polarographically with a Clark no. 5331 electrode (Yellow Springs Instruments) in a 53 YSI model (Simpson Electric Co) [30]. The chamber volume was 2 mL and the temperature was 28°. The amount of parasite used was equivalent to 2 mg of protein. In order to evaluate redox cycling, mitochondrial respiration was inhibited with 20 mM sodium cyanide. The $IC_{k_c50}$ equivalent concentration corresponds to the final concentration used in the oxygen uptake experiments. This concentration was calculated considering that the $IC_{k_c50}$ (culture growth experiments) was determined using $3 \times 10^6$ parasites/mL, equivalent to 0.0375 mg protein/mL as initial parasite mass; $80 \times 10^6$ parasites/mL, equivalent to 1 mg protein/mL, was used in the oxygen uptake experiments. In order to maintain the parasite mass-drug ratio constant in these two types of experiments, the original $IC_{k_c50}$ was corrected by this 26-fold parasite mass increase in the oxygen uptake experiments. Values are expressed as mean ± SD for three independent experiments. No effect of DMSO alone was observed.

*2.8.3. HPLC glutathione and trypanothione measurement*

To form glutathione and trypanothione fluorescent derivatized adducts, Tulahuén strain epimastigotes, equivalent to 1 mg protein, were suspended in 40 mM HEPPS, 2 mM EDTA buffer, pH 8, with 2 mM monobromobimane and incubated at 70° for 5 min. To precipitate proteins, 4 M methanesulfonic acid was added. After 10 min incubation at 4°, the sample was centrifuged at 10,000 *g* for 3 min. A 20 mL sample was applied to a Lichrospher 100 RP-1 8 (5 μm) reverse phase column and eluted during 60 min at a 1 mL/min flow. The eluting gradient was: 0–20 min, 90% of solvent A (0.25% w/v lithium α-camphorsulfonate, pH 2.35) and 10% solvent B (25% w/v 1-propanol in solution A); 20–40 min, linear gradient of 10–50% solvent B; from 40 to 60 min, 50% solvent B isocratic in solvent A, returning to initial conditions in 30 min. All measures were performed using a Merck-Hitachi high-pressure chromatograph L-6200 Intelligent Pump, with a F-1050 fluorescence detector and a D-2500 integrator. Emission and excitation wavelengths were 480 and 385 nm, respectively. The method detects reduced free thiols, but not disulfides [31].

*2.8.4. Statistical analysis*

Lineal regression analysis, correlation analysis, and ANOVA and Dunnett's multiple comparison tests were performed using Prism GraphPad software (GraphPad Software Inc.).

*2.8.5. Electrochemical measurements*

Mixed media cyclic voltammetry (DMF:citrate buffer/60:40) was performed employing KCl 0.3 M and ITBA 0.1 M, pH = 9, as support electrolytes. A three-electrode BAS 50 W potentiostat system was employed using a mercury drop, Ag/AgCl, and platinum wire as working, reference and auxiliary electrodes, respectively [32,33]. The solutions were degassed with nitrogen for 10 min before each measurement at 25°.

*2.8.6. Determination of $k_2$ the second-order decay rate constant of the nitro radical anion*

The return to forward peak current ratio $I_{pa}/I_{pc}$ for the reversible first electron transfer ($RNO_2/RNO_2^{\bullet -}$) is measured for each cyclic voltammogram, varying the scan rate from 0.1 to 10 V/s according to the procedure previously described [34]. Then a theoretical approach is applied to determine $k_2$ value which involve the drug concentration in the radical stability [35].

## 3. Results and discussion

The nitroheterocyclic agents employed in this study are grouped into three different chemical families (Fig. 1): (i) 2-nitroimidazoles (benznidazole as prototype), (ii) 5-nitroimidazoles (megazol as prototype), and (iii) nitrofurans (nifurtimox as prototype). The $IC_{k_c50}$ values for each drugs and strain are given in Table 1. All drugs tested

Table 1
Culture growth inhibition by nitro derivative compounds

| Drug | $IC_{k_c50}$ | | |
|---|---|---|---|
| | Tulahuén (μM) | LQ (μM) | Brener (μM) |
| Benznidazole | 11.44 ± 0.1 | 16.95 ± 0.7 | 12.77 ± 1.1 |
| RO150216 | 10.53 ± 1.3 | 10.30 ± 1.1 | 10.01 ± 0.4 |
| Megazol | 3.75 ± 0.1 | 4.24 ± 0.6 | 2.91 ± 0.2 |
| 1 | 38.11 ± 0.1 | 67.30 ± 2.9 | 32.27 ± 2.7 |
| 2 | 7.46 ± 0.3 | 10.29 ± 0.1 | 7.44 ± 0.7 |
| 3 | 34.16 ± 2.9 | – | 31.16 ± 0.5 |
| Nifurtimox | 9.91 ± 0.2 | 12.28 ± 0.2 | 10.44 ± 0.3 |
| 4 | 74.99 ± 1.3 | >100 | 80.17 ± 6.0 |
| 5 | 12.26 ± 6.0 | 20.16 ± 2.1 | 13.13 ± 0.7 |

The $IC_{k_c50}$ values for each drug compound studied in the Tulahuén, and LQ strains and clone Brener of *Trypanosoma cruzi*. Values are expressed as mean ± SD for three independent experiments. For details, see Section 2.

produced an inhibitory effect against *T. cruzi* epimastigotes, but differences in potency were observed. Megazol was the most potent, but only three times more potent than nifurtimox depending on the parasite strain used. The $IC_{k_c}50$ values were slightly higher for the LQ than for the Tulahuén strains or for the CL-Brener clone. The 2-nitroimidazole RO150216 shows growth inhibition potency similar to benznidazole. Albeit, it has a good inhibitory activity in the three strains tested. These results are consistent with previously reported *T. cruzi* strains susceptibility patterns [18,13].

The antichagasic drugs acts upon the nonreplicative trypomastigote and the intracellular amastigote forms. In this study we used the noninfective epimastigote form, as has been done in several other studies with other nitroimidazole and nitrofuran derivatives as well as other natural and synthetic potential trypanocidal agents, which have also proved to be efficient against the trypomastigote and amastigote forms [36]. Moreover, the epimastigote form is a suitable model for studying the mode of action of the compounds employed in the present study. Since the low molecular weight thiol content in the trypomastigote and amastigote forms of *T. cruzi* is lower than in the epimastigote form [14], should render these compounds more effective in the infective and intracellular replicative forms.

It has been proposed that nifurtimox and, possibly, benznidazole, can induce redox cycling, which could explain their toxic effects, through the production of superoxide radical anion and then hydroxyl radicals. To evaluate this possibility, we performed oxygen uptake experiments with or without cyanide, which is a mitochondrial respiration inhibitor. Table 2 shows Tulahuén epimastigote oxygen uptake, with or without 20 mM sodium cyanide, in the presence of $IC_{k_c}50$ equivalent drug concentration. When compared with controls, only nifurtimox and derivatives **4** and **5** produced an increase of oxygen uptake, more visible upon cyanide inhibition, indicating a clear redox cycling ($P < 0.01$). Megazol, benznidazole and its derivatives, did not have any effects on redox cycling as previously reported [2,37].

In contrast, megazol and drugs **2** and **3** inhibited oxygen uptake ($P < 0.01$) in a time-dependent fashion (Fig. 2). 2-Nitroimidazoles did not modify the epimastigote oxygen uptake. Similar results were found with other strains (data not shown). It is important to note that the use of $IC_{k_c}50$ equivalent drug concentrations validates a possible relationship between oxygen redox cycling or respiration inhibition with the parasite growth inhibition.

Reduction cathodic peak potential ($E_{pc}$, Table 2) indicate one-electron transfer to nitro groups to form nitro-anion radicals, while $k_2$ values (Table 2) indicate radical decay, that is, its stability, according to:

$$RNO_2 + e \xrightarrow{E_{pc}} RNO_2^{\bullet -}$$

$$2RNO_2^{\bullet -} + 2H^+ \xrightarrow{k_2} RNO_2 + RNO + H_2O$$

Under anaerobic conditions, the electrochemically formed anion radical dismutates more rapidly in the 5-nitroimidazole group of megazol than in the nitrofuran of nifurtimox, whereas 2-nitroimidazoles show intermediate dismutation kinetics (Table 2). Thus, there may be a relationship between the biological activity of megazol and nitroso derivative formation, which is reflected here through dismutation (Table 2).

There was no correlation between electrochemical potential and growth inhibition. However, the electrochemical potentials of nitrofurans (Table 2) were directly correlated with oxygen uptake under mitochondrial respiratory inhibition by cyanide (Pearson's correlation coefficient −0.99). This is in agreement with their redox

Table 2
Nitroderivatives: effect upon oxygen uptake, redox cycling, bioavailability, electrochemical potential and dismutation ability

| Drug | Respiration[a,b] | Oxygen redox cycling[a,b,c] | Bioavailability | Cyclic voltammetry | |
|---|---|---|---|---|---|
| | | | Log $P$[d] | $E_{pc}$[e] (mV) | $k_2$[f] (L/mol/s) |
| Control | 31.3 ± 1.7 | 2.1 ± 0.5 | | | |
| Benznidazole | 26.6 ± 7.9 | 2.3 ± 0.1 | 1.2 | −730 | $8.9 \times 10^2$ |
| RO150261 | 29.0 ± 5.5 | 1.5 ± 0.1 | 0.93 | −740 | $7.0 \times 10^2$ |
| Megazol | 18.3 ± 2.1** | 0.5 ± 0.5* | 0.22 | −733 | $1.9 \times 10^3$ |
| 1 | 28.1 ± 0.4 | 1.2 ± 0.5 | −0.37 | −742 | $7.8 \times 10^2$ |
| 2 | 26.2 ± 5.7* | 1.9 ± 0.3 | 0.17 | −758 | $3.3 \times 10^3$ |
| 3 | 8.2 ± 0.5* | 2.4 ± 0.3 | 1.69 | −753 | $2.7 \times 10^3$ |
| Nifurtimox | 40.0 ± 0.8** | 4.0 ± 1.5** | −0.34 | −630 | $5.3 \times 10^1$ |
| 4 | 26.2 ± 3.7* | 6.0 ± 0.4** | −0.42 | −617 | $2.3 \times 10^2$ |
| 5 | 34.1 ± 6.0 | 6.6 ± 0.2** | 0.23 | −594 | $8.9 \times 10^2$ |

The values correspond to the mean ± SD of three independent experiments. For details, see Section 2.
[a] Final drug concentrations used correspond to the $IC_{k_c}50$ equivalent concentrations as defined in Section 2.
[b] Respiration and oxygen uptake values are expressed as nanoatoms-gram of oxygen/min/mg protein.
[c] Sodium cyanide (20 μM) was added as well as the respective drug at the $IC_{k_c}50$ equivalent concentration.
[d] Bioavailability is expressed as log $P$, calculated using the demo SRC's LogKow (KowWin) Program software [40].
[e] $E_{pc}$ corresponds to the reductioncathodic peak potential expressed as milivolts and measured as described in Section 2.
[f] Dismutation constant ($k_2$) is expressed as L/mol/s. See Section 2.
* Dunnett's multiple comparison test: $P < 0.05$; ** Dunnett's multiple comparison test: $P < 0.01$.

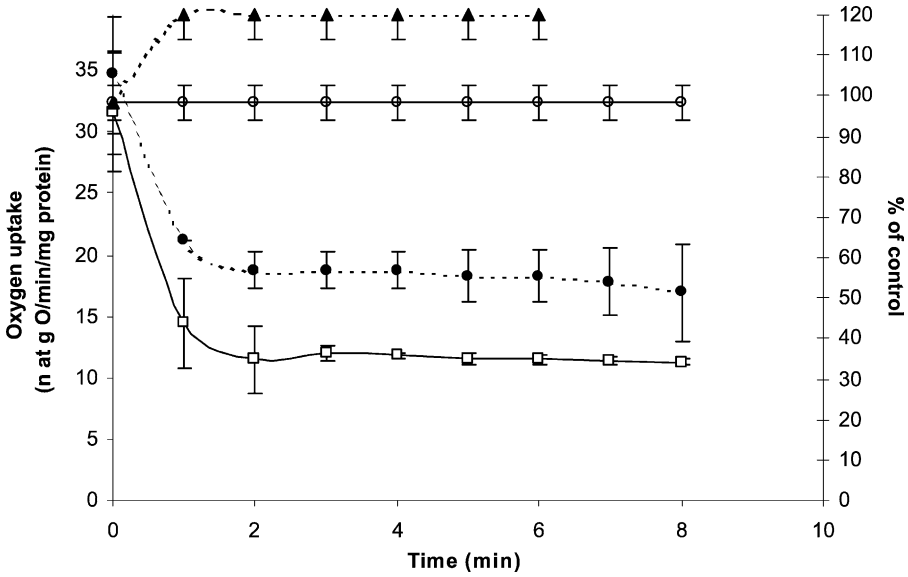


Fig. 2. Time effect of prototype nitroderivatives upon *T. cruzi* epimastigotes, Tulahuén strain respiration. Control (continuous line, open circles), nifurtimox (dotted line, closed triangles), megazol (dotted line, closed circles), drug **3** (continuous line, and open squares). Drug **2** (not shown) followed the same pattern than drug **3**. Values correspond to mean ± SD of three independent experiments and expressed as nanoatom gram of oxygen/min/mg protein. Percent variation with respect to the control is shown in the right axis.

cycling behavior. Considering that megazol and its derivatives are poor oxygen redox cyclers and their respiration inhibitory effect is time-dependent (Fig. 2), it may be assumed that their action is mediated by electrophilic metabolites; based on their faster dismutation ($k_2$ values, Table 2) and possibly also through a second electron transfer to the primary radical anion. This greater ability of megazol to form the nitroso species more rapidly than nifurtimox has also been shown using another technique, pulse radiolysis [38]. Such electrophilic metabolites may bind to epimastigote intracellular macromolecules. To test this, we determined the intracellular glutathione (GSH) and trypanothione ($T(SH_2)$) thiol contents of the Tulahuén strain.

In the presence of $IC_{k_c50}$ equivalent concentrations, megazol elicited a progressive decrease of the thiol content in 2 hr (Fig. 2), with a half-life of 88 min for $T(SH)_2$ (regression coefficient 0.85). GSH did not decrease as much as $T(SH)_2$, and its half-life was >200 min. All the tested nitroheterocyclic compounds induced a decrease of thiol content; $T(SH)_2$ was more affected than GSH (Fig. 4). The ability of nitrofurans to decrease thiols was comparable to that of nifurtimox, as previously reported [14,39], and to that of 2-nitroimidazoles and benznidazole as shown in the present paper. Moreover, the RO150216 compound presented a very high thiol scavenging capacity compared with all the compounds tested. However, it is similar to benznidazole's thiol scavenging capacity [14]. In general, RO150261 behaves similarly as benznidazole in growth inhibition potency, respiration inhibition and dismutation capacity as well as bioavailability. No difference in GSH content was observed when **4** and **5** were compared to controls ($P > 0.05$).

When homogenates of drug-treated parasites were incubated with an active *T. cruzi*'s trypanothione reductase preparation and further derivatized with monobromobimane followed by separation of the reaction products by HPLC, no significant increase in the reduced thiol concentrations shown in Fig. 4 was observed. Thus, indicating that the loss of reduced thiols was not due to oxidation, but rather to conjugation with electrophilic metabolites [14]. Appropriate controls showed no trypanothione or glutathione degradation by *T. cruzi* homogenates.

Nifurtimox can produce anion radicals and interfere with oxygen metabolism, as shown in Fig. 2. Megazol has a more complex behavior. In the first place, it inhibits mitochondrial respiration in a time-dependent fashion, and does not induce an increase in oxygen uptake, even when tested with cyanide. Second, it produces considerable depletion of $T(SH)_2$ and to a lesser extend, of GSH (Fig. 3). The same trend has been seen in other strains (data not shown). Finally, comparison of results obtained with the similar compounds, megazol and **1** reveals another important feature: the bioavailability of the drug.

Indeed both of these compounds have similar properties with respect to their ability to produce the nitroso form by dismutation; compound **1** appears to be an even more efficient thiol scavenger than megazol (Fig. 4). By contrast, megazol is at least 10 times more efficient with respect to inhibition of culture growth than compound **1** (Table 1). Actually, the only structural difference between the two compounds is the replacement of an oxygen atom in **1** by a sulfur atom in megazol; this change is enough to raise the log $P$ value from −0.37 for compound **1** to 0.22 in megazol [40] (Table 2). It is well known that compounds with negative log $P$ values cross cell membranes very poorly [41].

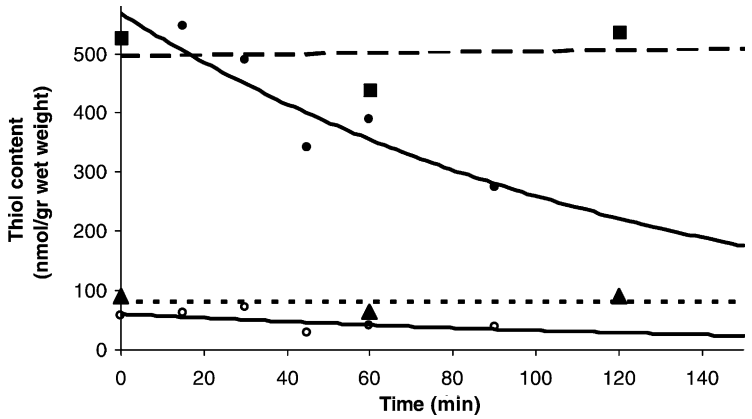


Fig. 3. Effect of megazol upon thiol content in *T. cruzi* epimastigotes. Reduced trypanothione $T(SH)_2$ regression coefficient 0.85, $P < 0.05$; controls and GSH-megazol regression coefficients <0.5, $P > 0.05$. Trypanothione half-life is 88 min. $T(SH)_2$ control (■), $T(SH)_2$ megazol (●), GSH control (▲), GSH-megazol (○).

A specific feature of megazol might therefore be related to its greater bioavailability. As for compounds **2** and **3**, which also have positive log *P* values (0.17 and 1.69, respectively), compound **2** is a prodrug of megazol after hydrolysis of the acetyl group, whereas compound **3** is not since the trifluoroacetyl group is only poorly hydrolyzed by cytosolic peptidases (not shown).

In conclusion, this work sheds some light on the differences between nitrofurans, exemplified by nifurtimox and nitroimidazoles, with megazol as a representative structure. Whereas the former compounds are essentially active as redox cycling agents, leading to oxidative stress (upper part on Fig. 2), the 5-nitroimidazoles are converted to the nitroso form, resulting from dismutation, as shown here, possibly also *via* a second one-electron reduction (lower part in Fig. 2). The resulting electrophilic species are efficient thiol scavengers, particularly for $T(SH)_2$, the cofactor of the detoxification enzyme trypanothione reductase, which has been shown to be essential for the survival of the trypanosome [42].

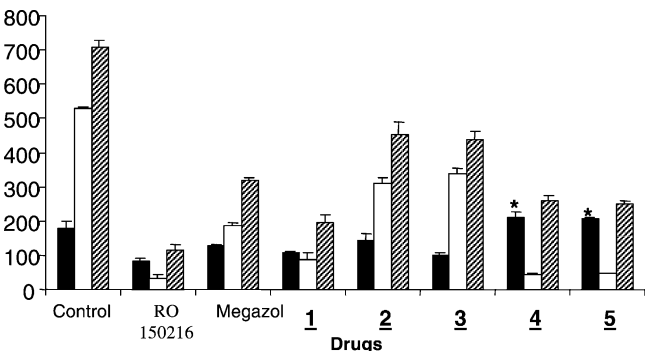


Fig. 4. Effect of nitroderivatives upon GSH (black bars), $T(SH)_2$ (white bars), and total thiol (scattered bars) content in *T. cruzi* epimastigotes, Tulahuén strain. Drug concentrations were equivalent to their respective $IC_{kc50}$, and the incubation time was 2 hr before thiol determination. Values are expressed as GSH nmol/g wet weight of parasites. Asterisks indicate no statistical difference with control in Dunnett's test.

Therefore, the action of both classes of compounds involves oxygen metabolism, in the case of nitrofurans by inducing oxidative stress, and by trypanothione depletion for nitroimidazoles.

Furthermore, the comparison of the effects produced by similar compounds suggests an additional feature responsible for the high efficacy of megazol, namely its suitable amphiphilic balance. On these grounds, other nitroimidazoles are currently under investigation, as well as the ability to act as thiol scavenger of host glutathione, toxicity and *in vivo* assays for the lead compound megazol.

## Acknowledgments

This research was supported in part by SIDA/SAREC, Fondecyt-Chile Grant Number 1000882 and 1020095, ECOS-Conicyt C98S01 and CNRS-Conicyt.

We thank professor Dr. Bruce Cassels for suggestions and critical review of the manuscript.

## References

[1] Moncayo A. Chagas' disease. Tropical disease research: progress 1991–1992. Geneva: WHO; 1993. p. 67–76.

[2] Castro JA, Diaz de Toranzo EG. Toxic effects of nifurtimox and benznidazole, two drugs used against trypanosomiasis (Chagas' disease). Biomed Env Sci 1988;1:19–33.

[3] Gorla NB, Ledesma OS, Barbieri GP, Larripa IB. Thirteen-fold increase of chromosomal aberrations nonrandomly distributed in chagasic children treated with nifurtimox. Mutat Res 1989;224:263–7.

[4] Filardi LS, Brener ZA. Nitroimidazole-thiadiazole derivative with curative action in experimental *Trypanosoma cruzi* infections. Ann Trop Med Parasitol 1982;76:293–7.

[5] Docampo R, Stoppani AOM. Generation of superoxide anion and hydrogen peroxide induced by nifurtimox in *Trypanosoma cruzi*. Arch Biochem Biophys 1979;1911:317–21.

[6] Docampo R, Moreno SNJ, Stoppani AOM, Leon W, Cruz FS, Villalta F, Muniz RFA. Mechanism of nifurtimox toxicity in different forms of *Trypanosoma cruzi*. Biochem Pharmacol 1981;30:1947–51.

[7] Docampo R, Moreno SNJ. Free-radical intermediates in the antiparasitic action of drugs and phagocytic cells. In: Pryor WA, editor. Free radicals in biology, vol. 6. Academic Press: New York; 1984. p. 243–88.
[8] Docampo R, Stoppani AOM. Generation of oxygen-reduction derivatives induced by nifurtimox and other nitrocompounds in *Trypanosoma cruzi*. Medicina (Buenos Aires) 1980;40(Suppl 1):10–6.
[9] Dubin M, Moreno SNJ, Martino EE, Docampo R, Stoppani AOM. Increased biliary secretion and loss of hepatic glutathione in rat liver after nifurtimox treatment. Biochem Pharmacol 1983;32:483–7.
[10] Moreno SNJ, Docampo R, Mason RP, Leon W, Stoppani AOM. Different behaviors of benznidazole as free radical generator with mammalian and *Trypanosoma cruzi* microsomal preparations. Arch Biochem Biophys 1982;218:585–91.
[11] Masana M, Toranzo EGD, Castro JA. Reductive metabolism and activation of benznidazole. Biochem Pharmacol 1984;33:1041–5.
[12] Diaz de Toranzo EG, Castro JA, Franke de Cazzulo BM, Cazzulo JJ. Interactions of benznidazole reactive metabolites with nuclear and kinetoplasmic DNA, proteins and lipids from *Trypanosoma cruzi*. Experientia 1988;44:880–1.
[13] Aldunate J, Morello A. Free radicals in the mode of action of antiparasitic drugs. In: Aruoma OI, editor. Free radicals in tropical diseases. Harwood Academic: Switzerland; 1993. p. 137–65.
[14] Maya JD, Repetto Y, Agosín M, Ojeda JM, Tellez R, Gaule C, Morello A. Effects of nifurtimox and benznidazole upon glutathione and trypanothione in epimastigote, trypomastigote, and amastigote forms of *Trypanosoma cruzi*. Mol Biochem Parasitol 1997;86:101–6.
[15] Berkelhammer G, Asato G. 2-Amino-5-(1-methyl-5-nitro-2-imidazolyl)-1,3,4-thiadiazole: a new antimicrobial agent. Science 1968; 1162:1146.
[16] Filardi LS, Brener Z. Susceptibility and natural resistance of *Trypanosoma cruzi* strains to drugs used clinically in Chagas disease. Trans R Soc Trop Med Hyg 1987;81:755–9.
[17] Bouteille B, Marie-Daragon A, Chauvière G, De Albuquerque C, Enanga B, Darde ML, Vallat M, Périé J, Dumas M. Effect of megazol in *Trypanosoma brucei brucei* acute and subacute infection in Swiss mice. Acta Trop 1995;60:73–80.
[18] Enanga B, Keita M, Chauvière G, Dumas M, Bouteille B. Megazol combined with suramin: a chemotherapy regimen which reversed the CNS pathology in a model of human African trypanosomiasis in mice. Trop Med Int Health 1998;3:736–41.
[19] Denise H, Mattews K, Lindergard G, Croft S, Barrett MP. Trypanosomiasis and leishmaniasis: between the idea and the reality of control. Parasitol Today 1999;15:43–5.
[20] Jennings FW, Chauvière G, Viodé C, Murray M. Topical chemotherapy for experimental African trypanosomiasis with cerebral involvement: the use of melarsoprol combined with the 5-nitroimidazole, megazol. Trop Med Int Health 1996;1:363–6.
[21] Viodé C, Bettache N, Narimantas C, Krauth-Siegel RL, Chauvière G, Bakalara N, Périé J. Enzymatic reduction studies of nitroheterocycles. Biochem Pharmacol 1999;57:549–57.
[22] De Castro SL, Meireles M. Mechanism of action of a nitroimidazole-thiadiazole derivative upon *Trypanosoma cruzi* tissue culture amastigotes. Mem Inst Oswaldo Cruz 1990;85:95–9.
[23] Ferreira RC, Ferreira LC. CL 64,855, a potent anti-*Trypanosoma cruzi* drug, is also mutagenic in the *Salmonella*/microsome assay. Mem Inst Oswaldo Cruz 1986;81:49–52.
[24] Borowy NK, Nelson RT, Hirumi H, Brun R, Waithaka HK, Schwartz D, Polak A. RO150216 a nitroimidazole compound active against human and animal pathogenic African trypanosomes. Ann Trop Med Parasitol 1988;82:13–9.
[25] Bouteille B, Chauvière G. Implication du mégazol dans la chimiothérapie des trypanosomoses. Med Trop 1999;59:321–30.
[26] Chauvière G, Viodé C, Périé J. Nucleophilic substitution studies on nitroimidazoles and applications to the synthesis of biologically active compounds. J Heterocyclic Chem 2000;37:119–26.
[27] Aldunate J, Ferreira J, Letelier MJ, Repetto Y, Morello A. *t*-Butyl-4-hydroxyanisole, a novel respiratory chain inhibitor. Effects on *Trypanosoma cruzi* epimastigotes. FEBS Lett 1986;195: 295–7.
[28] Ferreira J, Coloma L, Fones E, Letelier ME, Repetto Y, Morello A, Aldunate J. Effects of *t*-butyl-4-hydroxyanisole and other phenolic antioxidants on tumoral cells and *Trypanosoma* parasites. FEBS Lett 1988;234:485–8.
[29] Aldunate J, Traipe L, Spencer P, Morello A, Repetto Y. Effects of hydroquinones on intact *Trypanosoma cruzi* epimastigotes. Comp Biochem Physiol 1992;103C:97–100.
[30] Letelier ME, Rodriguez E, Wallace A, Lorca M, Repetto Y, Morello A, Aldunate J. *Trypanosoma cruzi*: a possible control of transfusion induced Chagas disease by phenolic antioxidants. J Exp Parasitol 1990;71:357–63.
[31] Fairlamb AH, Henderson GB, Bacchi CJ, Cerami A. In vivo effects of difluoromethylornithine on trypanothione and polyamine levels in bloodstream forms of *Trypanosoma brucei*. Mol Biochem Parasitol 1987;24:185–91.
[32] Núñez-Vergara L, Bollo S, Alvarez AF, Blázquez M, Squella JA. Nitro radical anion formation from nimodipine. Electroanal Chem 1993;345:121–34.
[33] Squella JA, Bollo S, de la Fuente J, Núñez-Vergara LJ. Electrochemical study of the nitro radical anion from nicardipine: kinetic parameters and its interaction with glutathione. Bioelectrochem Bioenergetics 1994;34:13–8.
[34] Bollo S, Nuñez-Vergara LJ, Bonta M, Chauvière G, Périé J, Squella JA. Cyclic voltammetric studies on nitro radical anion formation from megazol and some related nitroimidazole derivatives. J Electroanal Chem 2001;511:46–54.
[35] Olmstead ML, Nicholson RS. Cyclic voltammetry theory for the disproportionation reaction and spherical diffusion. Anal Chem 1969;41:862–4.
[36] Rodrigues Coura J, De Castro SL. A critical review on Chagas disease chemotherapy. Mem Inst Oswaldo Cruz 2002;97:3–24.
[37] Tsuhako MH, Alves MJ, Colli W, Brener Z, Augusto O. Restricted bioreductive metabolism of a nitroimidazole-thiadiazole derivative with curative action in experimental *Trypanosoma cruzi* infections. Biochem Pharmacol 1989;38:4491–6.
[38] Viodé C, De Albuquerque C, Chauvière G, Houée-Levin C, Périé J. Comparative study by pulse radiolysis of the radical anion derived from compounds used in Chagas' disease therapy. New J Chem 1997;21:1331–8.
[39] Repetto Y, Opazo E, Maya JD, Agosín M, Morello A. Glutathione and trypanothione in several strains of *Trypanosoma cruzi*. Effects of drugs. Comp Biochem Physiol 1996;115B:281–5.
[40] On-line interactive demo SRC's LogKow (KowWin) Program established by the Environmental Science Center, Syracuse Research Corporation, available on the Internet at: http://esc.syrres.com/interkow/logkow.htm [accessed 16 September 2002].
[41] Gago F, Alvarez-Builla J, Elguero J. Hydrophobicity measurements by HPLC: a new approach to *P* constants. J Liq Chromatogr 1987;10: 1031–47.
[42] Fairlamb AH, Cerami A. Identification of a novel thiol-containing cofactor essential for glutathione reductase activity in trypanosomatids. Mol Biochem Parasitol 1985;14:187–98.